Food Chemistry: X 19 (2023) 100813

Contents lists available at ScienceDirect

Food Chemistry: X

journal homepage: www.sciencedirect.com/journal/food-chemistry-x

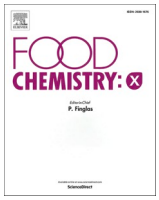

Hydro- and aerogels from quince seed gum and gelatin solutions

Saba Ahmadzadeh-Hashemi, Mehdi Varidi *, Majid Nooshkam

Department of Food Science and Technology, Faculty of Agriculture, Ferdowsi University of Mashhad (FUM), Mashhad, Iran

ARTICLE INFO

Keywords:
Protein-polysaccharide hydrogel
Quince seed gum
Gelatin
Composite aerogel
Rheological properties
Microstructure

ABSTRACT

The composite hydro/aerogels were designed using gelatin and quince seed gum (QSG) at total polymer concentration (TPC) of 1, 1.5 and 2% and gelatin/QSG ratio of 1:0, 1:0.5 and 1:1. The gel syneresis decreased significantly with increase in TPC and QSG. Although, hydrogels with 2% TPC had remarkably higher gel strength and elasticity than 1% TPC ones, the addition of high levels of QSG to the gelatin (i.e., gelatin/QSG 1:1) led to a decrease in its gel strength (~0.97-fold) and elasticity (~3,463-fold). The temperature-sweep test showed higher melting points in gelatin/QSG hydrogels (>60 °C) compared to the gelatin ones (~58 °C). Additionally, QSG addition to the gelatin led to more porous networks with higher gel strength, thermal stability, and crystallinity, as observed by scanning electron microscopy, differential scanning calorimetry, and X-ray diffractometer. Therefore, QSG could be used as a natural hydrocolloid to modify gelatin functionality.

1. Introduction

Hydrogels are considered versatile materials with a solid skeleton that is interpenetrated by water. They have received a great deal of research and industrial interest owing to their biocompatibility, proper release of bioactive molecules, high loading capacity and excellent mechanical properties. Hydrogels have a hydrophilic structure that is physically or chemically cross-linked, and also a great potential to trap a high volume of water or other biological liquids (Kazemi-Taskooh & Varidi, 2021).

Hydrogels convert to aerogels with minimum structural damages when the liquid phase is replaced with air. Aerogels have potential applications in various fields, such as adsorption and release of compounds (Mikkonen, Parikka, Ghafar, & Tenkanen, 2013), enzyme encapsulation (Buisson, Hernandez, Pierre, & Pierre, 2001) and smart packaging (de Oliveira et al., 2019). More importantly, food packaging industries have been recently motivated to use aerogels owing to their unique characteristics such as high surface area and porosity, ultra-low density and excellent thermal insulation and mechanical properties (Pan, Li, Chen, Zhang, & Zhang, 2021). Aerogel preparation requires two major steps (i) polymer gelation and (ii) gel drying (García-González, Uy, Alnaief, & Smirnova, 2012). The gelation conditions play a fundamental role in the structure of the resulting aerogel (Kleemann, Selmer, Smirnova, & Kulozik, 2018). The aerogel characteristics could be therefore predicted and controlled by identifying the relevant parameters that influence the properties of precursor hydrogel. Protein and polysaccharide-based hydrogels/aerogels are currently welcomed regarding amphiphilic nature, nutritional value, functional properties, biodegradability, biocompatibility and lower toxicity than synthetic polymers (Kazemi-Taskooh & Varidi, 2021).

Gelatin is one of the water-soluble hydrocolloidal polymers and a combination of different polypeptides, which can be obtained by the denaturation of the triple helix of collagen through acidic or alkaline hydrolysis. Gelatin chains are random coils in solutions at ambient temperature and turn into a helix and form a gel as the temperature decreases (Fennema, Damodaran, & Parkin, 2017). While gelatin is valued for its inherent flexibility and softness (Chandra & Shamasundar, 2015), it poses a challenge when it comes to the formation of gelatin hydrogels, as they typically require a higher polymer concentration (Kasapis, Mitchell, Abeysekera, & MacNaughtan, 2004). In addition, gelatin gels have certain limitations in terms of thermal stability (de Carvalho & Grosso, 2004) and turns into liquid in less than 10 min at 80 °C regardless of the gelatin concentration. This may be due to the low melting point of gelatin gel (Svetlana Rostislavovna Derkach, Ilyin, Maklakova, Kulichikhin, & Malkin, 2015). Hence, it necessitates the modification of the gelation properties of gelatin. One approach to enhance the gelation properties of gelatin is by incorporating polysaccharides, such as maltodextrin (Butler & Heppenstall-Butler, 2003), pectin (Gilsenan, Richardson, & Morris, 2003) and κ-carrageenan (Svetlana Rostislavovna Derkach et al., 2015). This improvement can be attributed to the effect of the simultaneous presence of two biopolymers in the complex structure. In binary combinations, the gelation rate is

* Corresponding author.
E-mail addresses: saba.ahmadzadeh@alumni.um.ac.ir (S. Ahmadzadeh-Hashemi), m.varidi@um.ac.ir (M. Varidi), nooshkamma@gmail.com (M. Nooshkam).

https://doi.org/10.1016/j.fochx.2023.100813
Received 4 March 2023; Received in revised form 15 July 2023; Accepted 24 July 2023
Available online 25 July 2023

typically higher and the critical concentration is lower compared to each component individually (Tolstoguzov, 1995).

Quince (*Cydonia oblonga*) is a native fruit of the west Asian region. Quince seed gum (QSG) is used in Iran to relieve cough and chest discomfort and to prevent asthma (Rezagholi et al., 2019). QSG is contained arabinose, xylose, galactose and glucose in proportion of 8:54:4:34 (Vignon & Gey, 1998). Thanks to its gelation properties, it is applied as a potential thickening agent for various applications (Guzelgulgen, Ozkendir-Inanc, Yildiz, & Arslan-Yildiz, 2021). QSG is a negatively charged polyelectrolyte with outstanding biocompatibility and biodegradability properties and higher molecular weight than xanthan, gellan, guar and locust beans (Rezagholi et al., 2019) and a higher swelling ratio than guar gum and galactomannan (Ashraf et al., 2017).

In the present research, it was hypothesized that the electrostatic interactions between cationic gelatin and anionic QSG in pre-hydrogel solution could modify the formation and properties of the gelatin/QSG composite aerogel. Thus, the hydrogel properties were evaluated by various techniques to characterize the interactions between gelatin and QSG, which would affect the physical properties of the composite aerogels. The resulting aerogels were then characterized by Fourier transform infrared spectroscopy (FTIR), scanning electron microscopy (SEM), X-ray diffraction (XRD), differential scanning calorimetry (DSC) and textural tests.

2. Materials and methods

2.1. Materials

Quince seeds were purchased from a local market (Mashhad, Iran). They were cleaned and packed in plastic bags and stored in a desiccator. Gelatin type B (Bloom range: 80–100) was acquired from Faravari Darooi Gelatin Halal Co. (Qazvin, Iran). Other chemicals were purchased from Merck Co. (Darmstadt, Germany) and Sigma-Aldrich Co. (St Louis, MO, USA).

2.2. Gum extraction

QSG was extracted according to a modified version of the hot water method (Farahmand, Varidi, & Koocheki, 2016). Briefly, seeds were stirred in distilled water (ratio of 1:32.5) at 47 °C for 3 h. Extracted mucilage was then separated with a Buchner funnel and precipitated by adding a volume of 96% ethanol three times greater than the volume of the gum. The obtained gum (QSG) was dried in an oven at 50 °C and then powdered, packed and stored at 4 °C. The gum contained 14.52% moisture, 71.62% carbohydrate, 8.13% ash, 4.02% fat and 1.71% protein.

2.3. Gelatin/QSG composite hydrogel

Preliminary experiments indicated that the pH in which gelatin and QSG have the highest difference charge was 5 (the zeta-potential values of gelatin and QSG at pH 5 were found to be 13 and −18 mV, respectively). The electrostatic attraction between QSG and gelatin could therefore lead to the formation of hydrogel structures. Thus, gelatin and QSG were dissolved in acetate buffer (pH 5; 25 mM) at 40 °C for 15 min, in different weight ratios of 1:0, 1:0.5 and 1:1 (gelatin/QSG) with 1%, 1.5% and 2% total polymer concentration (TPC). The solutions were then stored at 4 °C for 24 h to complete hydrogel formation.

2.4. Hydrogel characterization

2.4.1. Syneresis

The hydrogels were centrifuged (93×*g*, 5 min) and then stored upside down for 90 min at 25 °C. The following equation was finally used to calculate the syneresis of the composite hydrogels (Kazemi-Taskooh & Varidi, 2021):

$$\text{Syneresis}\ (\%) = \frac{\text{Expelled water (g)}}{\text{Hydrogel weight (g)}} \times 100 \quad (1)$$

2.4.2. Texture

A cylindrical probe (5 mm diameter) was used to penetrate the cylindrical hydrogels (20 × 10 mm) at a test speed of 1 mm s^{-1}, by a texture analyzer (Stable Microsystems, TA-XT plus, UK). The gel strength of the samples was measured from force-time curves.

2.4.3. Rheology

The rheological properties of the hydrogels were measured by a rheometer (MCR 302, Anton Paar, Austria). The strain sweep test was firstly performed at 1 Hz and 25 °C to determine the viscoelastic linear region, which was found to be 0.1%. The time sweep was then done at room temperature for 32 min and the changes in storage modulus (G') and loss modulus (G'') were recorded. Subsequently, the frequency sweep was performed at 0.1 % strain over the angular frequency range of 0.06–62.83 rad/s at 25 °C. The viscoelastic parameters (G' and G'') were calculated according to the Power-law equation (Kazemi-Taskooh & Varidi, 2021):

$$G' = K'\omega^{n'} \quad (2)$$

$$G'' = K''\omega^{n''} \quad (3)$$

$$\tan\delta = \frac{G''}{G'} \quad (4)$$

where K', n', K" and n" are the consistency index of G', flow behavior index of G', consistency index of G" and flow behavior index of G", respectively.

Moreover, the gel-sol transition was performed on the composite hydrogels to measure their melting temperature. The gels were heated from 5 to 60 °C and the temperature at the crossover of G' and G" during heating was recorded as the melting point (T_m) of the samples (Mohtar, Perera, Quek, & Hemar, 2013).

2.4.4. Color

The color indices L^* (lightness), a^* (greenness-to-redness) and b^* (blueness-to-yellowness) of the hydrogels were measured by a chromameter (Konica Minolta, C-410, Japan). A standard tile was used to calibrate the device and the color indices were then recorded to calculate the total color difference (ΔE) and browning index (BI) of the samples, as below (Nooshkam, Varidi, & Alkobeisi, 2022):

$$\Delta E = \sqrt{\Delta L^{*2} + \Delta b^{*2} + \Delta a^{*2}} \quad (5)$$

$$BI = \frac{\left(\frac{a^* + 1.75\ L^*}{5.645L^* + a^* - 3.012b^*}\right) - 0.31}{0.172} \times 100 \quad (6)$$

2.5. Aerogel formation via freeze-drying method

The aerogels were produced according to the Pan et al. (2021) method, with some modifications. The hydrogel samples were pre-frozen at −18 °C for 48 h. The frozen hydrogels were then freeze-dried (0.07 mW, −48 °C, 48 h) to fabricate aerogels.

2.6. Aerogel characterization

2.6.1. Morphology

The microstructural properties of aerogels were observed by an SEM apparatus (LEO, 1450VP, Germany) operated at 20 kV in which both the surface and cross-section of gold-coated samples (~cubes of 1 mm^3) were analyzed. The SEM pictures were then analyzed by ImageJ to

provide the total pore area and pore size of the samples.

2.6.2. Porous properties

The mass and volume of the aerogels were measured to calculate the bulk density (ρ_b). The skeleton density (ρ_s) of the samples was determined by a 50 mL pycnometer and hexane as the solvent. Finally, the following equation was used to calculate the porosity of the aerogels (Yun et al., 2017):

$$\text{Porosity}\,(\%) = \left(1 - \frac{\rho b}{\rho s}\right) \times 100 \quad (7)$$

2.6.3. Hygroscopicity

The method of Ahmadi, Madadlou, and Saboury (2016) was applied to determine the hygroscopicity of the aerogels, by measuring their moisture absorption capacity at 83.6% relative humidity (RH). The hydrogels were placed in a desiccator (83.6% RH, 30 °C) and weighed over time until a constant weight was reached. Then, the moisture sorption (MS) percentage of the samples was calculated as below:

$$\text{MS}\,(\%) = \frac{W - W0}{W0} \times 100 \quad (8)$$

where W is the aerogel weight after moisture sorption and W_0 denotes the initial weight of aerogel.

2.6.4. Textural studies

The penetration test was applied to measure the textural parameters of the aerogels. The method was followed according to Section 2.4.2.

2.6.5. Chemical structure

Infrared spectroscopy was performed to confirm the chemical structure of the aerogels. Pellets containing aerogel powder and potassium bromide (1:100 w/w) were prepared and analyzed by an FTIR device (Thermo Nicolet, AVATAR-370 FTIR, USA) at the wavenumber range of 4000–400 cm^{-1}.

2.6.6. Thermostability

The thermal properties of the aerogels were measured by a DSC apparatus (Linseis, PT 1000, German). About 2 mg of the samples were tested at a temperature range of 25 to 320 °C at a heating rate of 10 °C min^{-1}.

2.6.7. Crystallinity

The crystallinity of prepared samples was recorded using an X-ray diffractometer (EXPLORER, GNR, Italy) equipped with a Scintillator detector, using Cu Kα radiation (40 kV, 30 mA) in the range of $5° \leq 2\theta \leq 40°$ with an angle step of 0.02° and 1 s per step (Yadav, Mehrotra, Bhartiya, Singh, & Dutta, 2020).

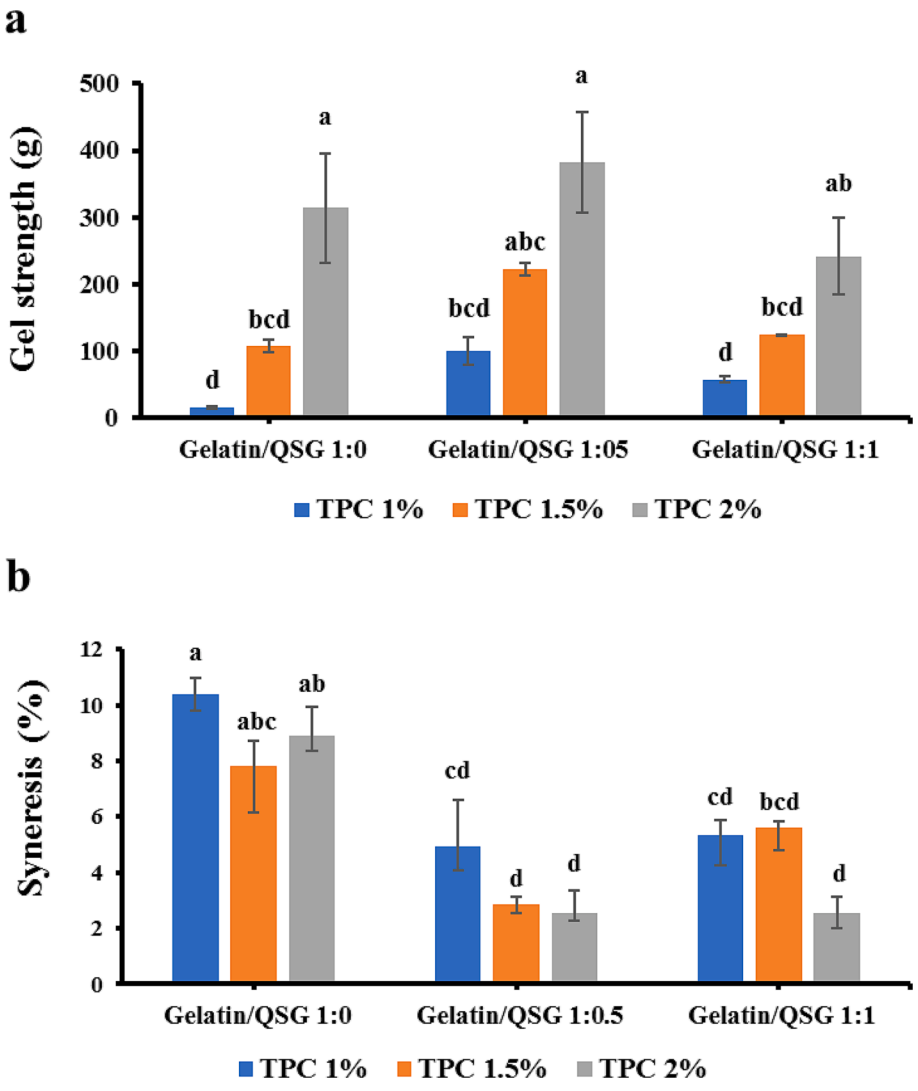

Fig. 1. Effect of gelatin/QSG ratio and TPC on gel strength (a) and syneresis (b) of the composite hydrogels.

2.7. Statistical analysis

The data were analyzed by Minitab software (version 19) using a completely randomized design in a factorial arrangement. The factors were gelatin/QSG ratio (1:0, 1:0.5 and 1:1) and TPC (1, 1.5 and 2%). The significant differences between the means were evaluated by the Tukey test at $p < 0.05$. The experiments were performed in three replicates.

3. Results and discussion

3.1. Gelatin/QSG composite hydrogels

3.1.1. Gel strength of hydrogels

The gel strength of the hydrogels was significantly influenced by TPC and gelatin/QSG ratio (Fig. 1a). It increased from 58.30 g to 312.86 g as the TPC raised from 1% to 2% ($p < 0.05$). It is noteworthy that the gel strength of the gel is affected by the structure of the gel network. An ordered three-dimensional structure could result in a harder structure than disordered structures (Liu et al., 2020). On this point, the improved gel strength may be due to the homogenous structure of the hydrogels as a consequence of TPC enhancement (Kazemi-Taskooh & Varidi, 2021), as confirmed by SEM micrographs (section 3.2.1). The gel strength of the hydrogels rose from 145.97 g to 235.38 g (~1.61-fold) as the gelatin/QSG ratio changed from 1:0 to 1:0.5 ($p < 0.05$), but further increase in QSG concentration (i.e., 1:1 gelatin/QSG) led to a lower gel strength of 141.57 g (~0.97-fold) compared to the gelatin hydrogel.

For a specific protein-polysaccharide ratio, there is an optimal ratio for which electrostatic interactions reach an equilibrium between associative and repulsive interactions, leading to the formation of the strongest gel (Le & Turgeon, 2013). In the present study, this ratio was found to be 1:0.5 gelatin/QSG ratio, which is the driving parameter of gel structure and properties. Indeed, as the content of anionic polysaccharides increases, it is possible that all positive charges on the gelatin molecules become neutralized. In addition, the presence of excess polysaccharide molecules could introduce more negatively charged groups into the system. Consequently, the resulting electrostatic repulsive forces between the anionic polysaccharide molecules may contribute to a reduction in the strength of the hydrogel (Wu, Degner, & McClements, 2014). In line with our study, Huang et al. (2021) reported that in excess gelatin, the gel's strength is dominated by gelatin-gelatin junctions, with some reinforcement from gelatin-anionic polysaccharide junctions; whilst, when gelatin concentrations are low, anionic polysaccharide-anionic polysaccharide associations become dominant, with some support from gelatin-anionic polysaccharide junctions. Similarly, it has been reported that gelatin concentrations above 0.3% reduced the gel strength of whey and egg white proteins (Babaei, Mohammadian, & Madadlou, 2019; Martin et al., 2016). Moreover, Binsi et al. (2017) demonstrated that the hardness value of fish gelatin gel increased in the presence of gum Arabic, xanthan gum, guar gum and tragacanth gum, mainly due to the introduction of more polymer junction zones. The authors claimed that the electrostatic interaction between anionic hydrocolloids and positive charges on the surface of gelatin could strengthen the gelatin network and minimize its syneresis (Binsi et al., 2017). Additionally, a greater hardness of the hydrogels could indicate increased crystallinity and reduced chain mobility (Zhang, Xia, & Zhao, 2012), as confirmed by XRD results (Section 3.2.6).

3.1.2. Syneresis

The binary hydrogels experienced a significant decrease in syneresis (9.04 to 3.44%) as the gelatin/QSG ratio decreased from 1:0 to 1:0.5 ($p < 0.05$); however, the syneresis value increased to 4.50% as the gelatin/QSG ratio was further decreased to 1:1 ($p > 0.05$) (Fig. 1b). By increasing TPC from 1% to 2%, syneresis decreased by an average of 32.15% ($p < 0.05$). The highest and lowest syneresis values were observed in 1% TPC-1:0 gelatin/QSG (~10.38%) and 2% TPC-1:0.5 gelatin/QSG (~2.54%), respectively. The lower syneresis of the hydrogels containing QSG and greater biopolymer concentrations could be due to their improved gel strength (Babaei et al., 2019b), elasticity (Kazemi-Taskooh & Varidi, 2021) and hydrophilicity (Pires Vilela, Cavallieri, & Lopes da Cunha, 2011). It has also been reported that the hydroxyl groups of polysaccharides with high affinity to water molecules could provide greater water holding capacity in protein-polysaccharide mixtures compared to protein-based structures (Babaei, Khodaiyan, & Mohammadian, 2019). This can be attributed to their capacity to bind water molecules together within the interstitial spaces, thereby lowering the syneresis (Binsi et al., 2017).

3.1.3. Rheological properties

3.1.3.1. Time sweep. The G' and G'' of the hydrogels increased continuously with time and then approximated to a plateau (data not shown). The moduli of the samples at the end of time sweep (32 min) were then recorded and compared (Table 1). The G' value for samples (with and without QSG) was greater than G'', which is a common characteristic of strong gels, mainly due to the high concentrations of helical structures in gelatin (Gómez-Guillén et al., 2002). As the TPC raised from 1% to 2%, G' and G'' increased from an average of 13082.6 Pa to 15889.75 Pa and 5414.55 Pa to 11057.25 Pa, respectively ($p < 0.05$). For gelatin/QSG 1:1, the G' was about 3-time greater than G'', but both moduli (G' and G'') values were less than those of gelatin gels (i.e., gelatin/QSG 1:0) ($p < 0.05$). This could be ascribed to the repulsive interactions between polysaccharide molecules at such concentrations that may prevent the network formation of protein gel (Sow, Nicole Chong, Liao, & Yang, 2018). This trend is largely supported by the gel strength results, as 2% TPC and gelatin/QSG 1:0 had higher gel strength compared to their counterparts (Fig. 1a).

3.1.3.2. Frequency sweep. Fig. 2a-b and Table 1 reveal the variation of G' and G'' of the gelatin/QSG composite hydrogels as a function of angular frequency. All hydrogels had flow behavior indices of $K > 0$ and $0 < n < 1$, demonstrating a pseudoplastic behavior (Table 1). Moreover, at all frequencies, G' of the hydrogels was higher than G'' (Fig. 2a-b), indicating a harder and elastic structure in the composite hydrogels (Derkach, Kuchina, Kolotova, & Voron'ko, 2020). In addition, the loss tangent of the hydrogels was below unity (Fig. 1S), which is an indication of solid-like behavior in the samples (Bashash, Varidi, & Varshosaz, 2022).

Worthy to note that the frequency dependence of G' and G'' could indicate the type of structure in the hydrogels. Therefore, the frequency sweep data were fitted by the Power-law model to quantitatively analyse the G'- and G''-frequency dependence degree of the mixed gels (Table 1). By increasing TPC from 1% to 2%, K'' and K' increased by an average of 1.88 and 1.3 times, respectively ($p < 0.05$). The slope of the Power-law equation, represented by the parameter K, provides insights into the rheological behavior of the hydrogel samples. In this study, it was observed that as the slope (K) increases, indicating a higher degree of shear thinning behavior, the transition from a solid-like state (K') to a liquid-like state (K'') or vice versa occurs more rapidly. This finding aligns with the findings reported by Abebe and Ronda (2014), who also noted a similar relationship between the slope of the Power-law equation and the transition from semi-solid to semi-liquid behavior. Therefore, the increase in K values with increasing TPC in the current study suggests that the hydrogel samples experience faster transitions between semi-solid and semi-liquid states as the polymer concentration rises.

As the TPC increased from 1% to 2%, average of n' and n'' values of the composite hydrogels increased from 0.5406 to 0.6449 and 0.5897 to 0.5956, respectively ($p < 0.05$) (Table 1). Since n indicates the relation between moduli of the frequency functions, it can be concluded that the behavior tends to be elastic in the composite gels. This could be ascribed to the formation of junction zones between gelatin and polysaccharide,

Table 1
Rheological properties of gelatin and gelatin/QSG composite hydrogels.

TPC (%)	Gelatin/QSG ratio	Time sweep		Frequency sweep				Temperature sweep T_m (°C)
				G'		G"		
		G' (Pa)	G" (Pa)	K' (Pa.s^n)	n'	K" (Pa.s^n)	n"	
1	1:0	26159.5 ± 0.707^b	10827.5 ± 3.54^b	15305 ± 3.54^b	0.1462 ± 0.000212^c	5879.5 ± 0.354^b	0.1683 ± 0.00177^d	58.5 ± 0.707^a
	1:1	5.7 ± 0.063^d	2.1 ± 0.156^d	0.1031 ± 0.019^c	0.9352 ± 0.000283^b	0.0074 ± 0.000283^c	1.0111 ± 0.00014^a	> 60
2	1:0	31005.5 ± 7.78^a	21881.5 ± 2.12^a	19331 ± 1.41^a	0.1468 ± 0.000212^c	11014 ± 0.707^a	0.1951 ± 0.000141^c	58 ± 0.0^a
	1:1	774 ± 0.070^c	233 ± 0.00^c	9.8797 ± 0.156^c	1.1429 ± 0.00007^a	0.9585 ± 0.0354^c	0.9961 ± 0.00014^b	> 60

Means within the same column with different superscripts differ significantly ($p < 0.05$).

leading to higher G' and gel strength in the hydrogels (Svetlana R. Derkach et al., 2020). These findings are highly supported by the gel strength observations of the hydrogels (Fig. 1a); indeed, the higher the TPC, the greater the gel strength and elasticity.

Reducing ratio of gelatin/QSG from 1:0 to 1:1 increased n' (~7.09-fold) and n'' (~5.52-fold) of the hydrogels ($p < 0.05$). More importantly, 1:1 gelatin/QSG hydrogels had significantly lower K' (~3,463-fold) and K'' (~17,597-fold) compared to the 1:0 gelatin/QSG counterparts. In congruent with our observations, Lee et al. (2003) noticed that as the ratio of gellan increased up to 60% in the gellan/gelatin mixed systems, the elastic property was enhanced mainly due to the existence of interpenetrating networks or association between two biopolymers; while, further increase in gellan content led to a system with remarkably lower elastic modulus.

3.1.3.3. Temperature sweep. The temperature sweep test was applied to measure the melting temperature of the hydrogels (Fig. 2c-d and Table 1). The G' and G'' of the hydrogels (with and without QSG) increased slightly as the temperature increased to 50 °C and the G' was greater compared to the G'', which shows that the hydrogels remained gelled. Further increase in temperature resulted in a markedly decrease in both G' and G'' values and this trend was more pronounced in the G' profile. The G' and G'' cross over at some point; therefore, the critical temperature at which G' = G'' is defined as the melting point/temperature (T_m) of the gel (Mohtar et al., 2013). Above T_m, G'' becomes greater than G', which demonstrates gel-to-liquid state transition.

As can be observed from Fig. 2c, the T_m values of gelatin/QSG 1:0 with 1% and 2% TPC were calculated to be approximately 58.5 and 58 °C, respectively ($p > 0.05$). The reduction in G' led to a great loss in the network structure of the gelatin gels and the sample ultimately transformed into a viscous liquid at G'' > G', mainly due to the destruction of and or lower triple helical structure (Gómez-Guillén et al., 2002). However, no crossover was observed in the temperature sweep profile of gelatin/QSG composite hydrogels (Fig. 2d), indicating a solid-like behavior of the corresponding samples. This may be attributed to the improved thermal stability of the hydrogels, likely as a consequence of the interactions between protein and polysaccharide (Mohtar et al., 2013), as confirmed by FTIR (Section 3.2.3) and DSC (Section 3.2.4) results. Although, the gelatin/QSG 1:1 hydrogel had lower gel strength and elasticity compared to the gelatin/QSG 1:0 counterpart, the higher T_m of the former could be mainly due to ability of polysaccharides to increase the thermal stability of proteins through macromolecular

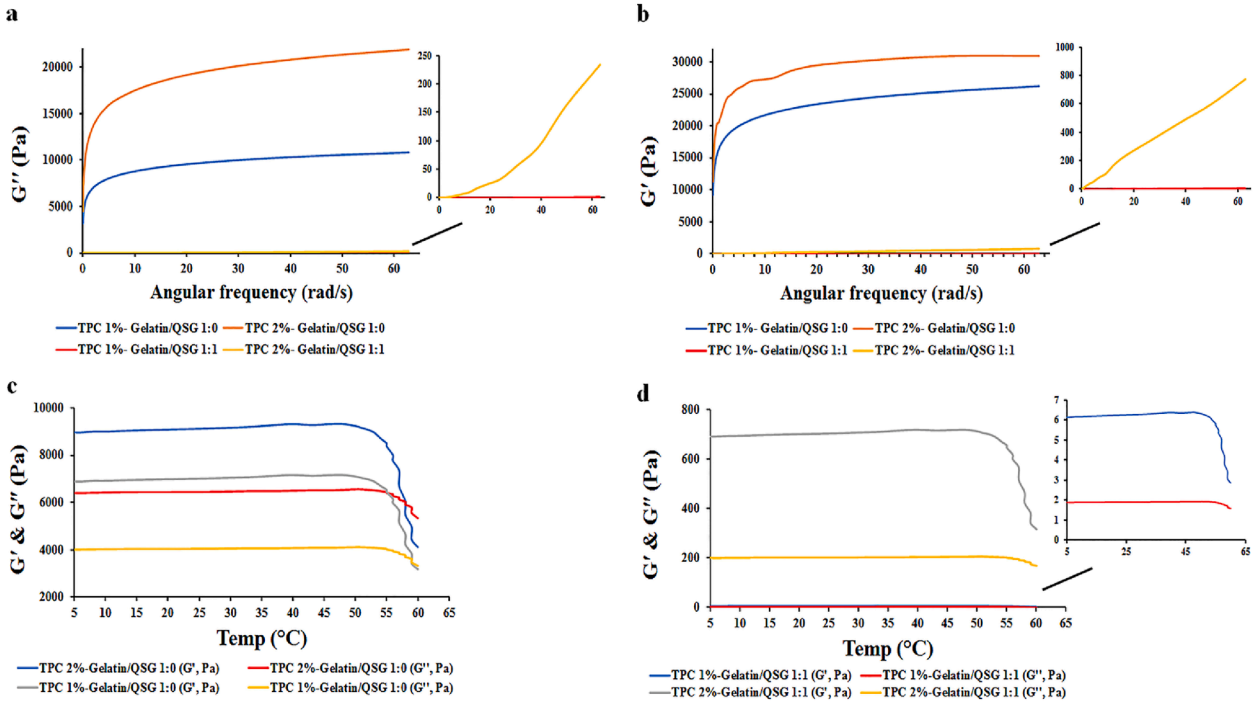

Fig. 2. Loss (a) and storage (b) moduli of gelatin/QSG hydrogels as a function of angular frequency. Loss and storage moduli of gelatin/QSG hydrogels as a function of heating temperature (c and d).

crowding effect. The crowding agent can reduce the protein's solvent availability and force the protein to adopt a compact and steady-state structure, and precipitation is therefore prevented during thermal treatment (Sasahara, McPhie, & Minton, 2003). The increased thermal stability of gelatin in the presence of gellan and carrageenan has been reported in some studies (Fonkwe, Narsimhan, & Cha, 2003; Varghese, Chellappa, & Fathima, 2014).

3.1.4. Color

Color reflects the sensory and quality attractiveness of versatile food products and it is, therefore, one of the essential factors in the food sections. The color indices of the composite hydrogels are provided in Table 1S. The addition of QSG to gelatin solutions led to composite hydrogels with significantly lower L^* and higher b^*, a^* and BI, compared to the gelatin hydrogels. The TPC had a similar effect on the color indices of the gels and the 2% TPC-based mixed gels were generally darker than the 1% TPC-based ones ($p < 0.05$). This behavior might probably be attributed to the presence of phenolic compounds in the QSG, which can absorb light at lower wavelengths and provide more yellowish and brownish hydrogels (Nooshkam et al., 2022). It is also necessary to note that gels with less cross-linked and packed networks may have lower light scattering ability (Acar & Kurt, 2020). On this point, the lower lightness of the composite hydrogels could be highly attributed to their greater porosity. Moreover, all hydrogels experienced an increase in ΔE with increasing TPC and decreasing gelatin/QSG ratio and the overall color change of the composite hydrogels was very distinct (ΔE > 3). Accordingly, Petcharat and Benjakul (2017) demonstrated that the addition of gellan to the fish gelatin provided mixed gels with lower L^* and higher a^* and ΔE compared to the gelatin gels.

3.2. Gelatin/QSG composite aerogels

3.2.1. Morphology and porosity

The bulk density of the aerogels was in the range of 0.016 to 0.021 g cm^{-3}. In line with our results, the bulk density of 0.068–0.168 g cm^{-3} was reported for hydrophobic gelatin-silica composite aerogels (Yun et al., 2017). The network structure of gelatin/QSG composite aerogels was investigated by SEM and the results are provided in Fig. 3a. As can be observed, the gelatin/QSG aerogel matrices were porous, with a three-dimensional interconnected microstructure. Furthermore, the addition of QSG to the gelatin led to a more porous network with weaker walls than the gelatin aerogels. In this context, the number of pores and their total area and porosity of the aerogels were measured and provided in Fig. 3b-d. As the TPC increased from 1% to 2%, the number of pores and the total area of pores increased significantly by an average of 36.59% and 71.75%, respectively. This might be ascribed to the associative interactions between gelatin and QSG molecules with the increase of TPC. The pore's number and area were also influenced markedly by the gelatin/QSG ratio. Lowering gelatin/QSG ratio from 1:0 to 1:1 resulted in a significant decrease in the number of pores (~32.45%) and an increase in their mean area (~160.49%), most probably due to the repulsive forces between QSG molecules at excess anionic polysaccharide content. It could be therefore concluded that QSG likely increased the porosity of the aerogels. As mentioned previously, reducing the gelatin/QSG ratio from 1:0 to 1:1 decreased gel strength and elasticity, which was in line with the porosity of the hydrogels/aerogels. These results are supported by the porosity data (Fig. 3d). The gelatin/QSG aerogels with 2% TPC had higher porosity compared to those containing 1% TPC (~8.32%). Moreover, the porosity of aerogels obtained from the 1:1 gelatin/QSG ratio was higher than the gelatin aerogels (~9.78%). In congruent with our research, Varghese et al. (2014) reported that the addition of carrageenan to gelatin hydrogels increased their porosity remarkably. The interconnected pores of the gelatin/QSG aerogels can allow an efficient nutrient (bioactive) transfer and gaseous exchange in food and tissue engineering applications.

3.2.2. Hygroscopicity

The aerogels with porous structures could absorb water from humid air and the extent of water absorption is dependent on the aerogel

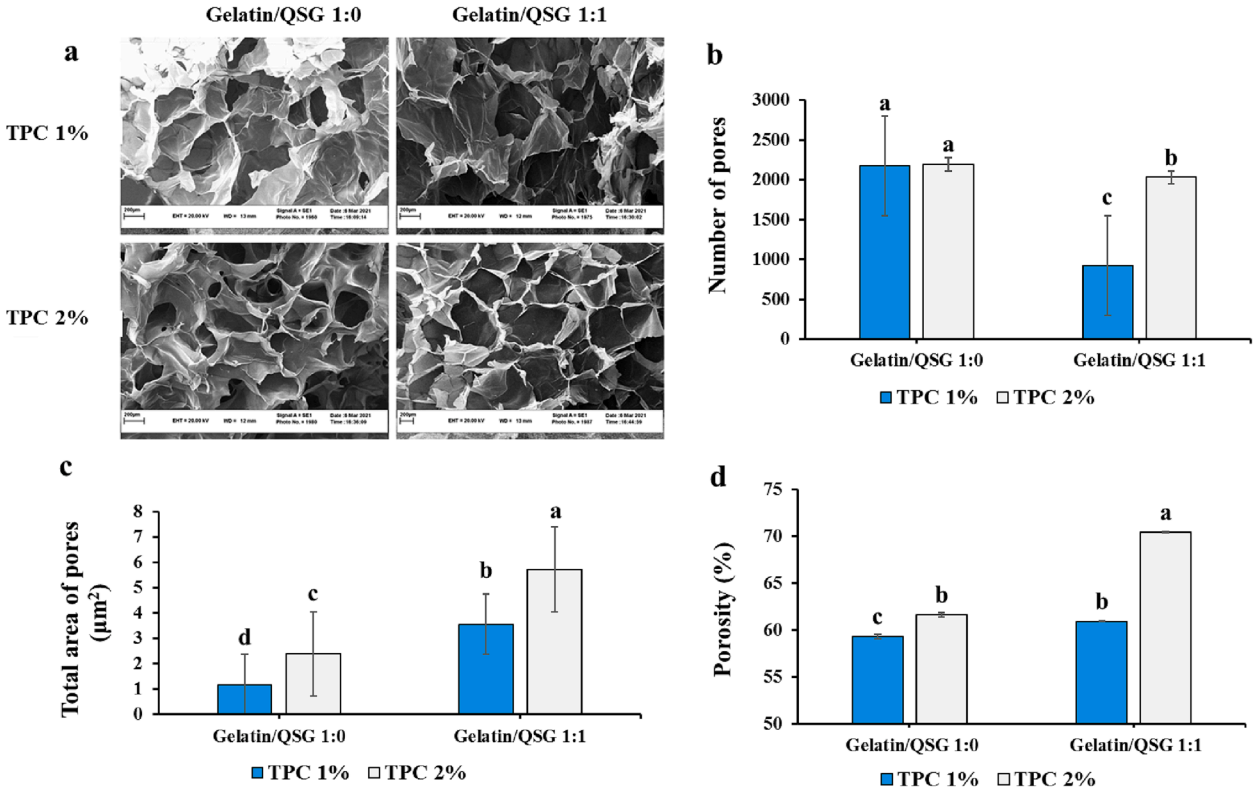

Fig. 3. Microstructure (a), number of pores (b), total area of pores (c), and porosity (d) of gelatin/QSG aerogels.

composition (Arboleda et al., 2013). Fig. 4a illustrates the moisture sorption kinetics of gelatin/QSG composite aerogels determined at 83.6% RH. The aerogels experienced maximum moisture sorption within the first 24 h, mainly due to their inherent hygroscopicity. The moisture sorption was then decreased and finally reached constancy. At first glance, gelatin aerogel with 1% TPC had the highest moisture absorption rate. But what is important about moisture absorption here is the amount of water trapped in the holes. This sample had low gel strength and high syneresis and during the investigation of moisture absorption, it had an unstable structure and the seeped water was easily seen. The gelatin/QSG aerogels had also remarkable moisture sorption within the first 24 h, likely due to the high tendency of QSG to water sorption (Ghadermazi, Khosrowshahi Asl, & Tamjidi, 2019). The reason behind the water uptake from the air by the gelatin/QSG aerogels is probably due to the affinity of both gelatin and QSG for water (Ghadermazi et al., 2019; Sun et al., 2022). Moreover, the high moisture sorption of the aerogels has been attributed to their high specific surface area (Ahmadi et al., 2016). For a more detailed examination on the moisture sorption behavior of gelatin/QSG aerogels, a specific surface area test should be used in future studies.

3.2.3. FTIR spectroscopy

Fig. 4b-c show the FTIR spectra of gelatin, QSG and composite aerogels. The peaks at 1645.59, 1543.77 and 1300–1200 cm^{-1} in the gelatin spectrum (Fig. 4b) were assigned to Amide I (C—O stretching vibration with minor contributions of C—N stretching), II (N—H deformation) and III (C—N stretching and N—H deformation), respectively (Nooshkam & Varidi, 2020). Moreover, the peaks at 3457.66 cm^{-1} and 3285 cm^{-1} in the gelatin spectrum was attributed to O—H stretching vibration of water molecules and N—H stretching vibrations, respectively (Bashash et al., 2022).

The QSG spectrum (Fig. 4b) revealed an intense broad band at ~3417.07 cm^{-1}, which was related to O—H stretching modes (Kačuráková, Capek, Sasinková, Wellner, & Ebringerová, 2000). The vibrations associated with stretching of C—H bonds of QSG can be identified by the bands occurring approximately at 2800–3000 cm^{-1} (Wang et al., 2018). The wavenumber range of 1620–1420 cm^{-1} was ascribed to C═O stretches in carbonyl groups of uronic acid residues (Manrique & Lajolo, 2002). Also, the peaks at about 1425 cm^{-1} and 1051 cm^{-1} could be related to the C-OH bending and C—O (glycosidic linkage) stretching vibrations, respectively (K. Chen & Zhang, 2019). The absorption band of 1425 cm^{-1} might also be related to the carboxylate anions (COO^-) stretching vibration (Nooshkam et al., 2022). Moreover, the sharp peak at around 1614 cm^{-1} might be ascribed to the stretching vibration of ester (K. Chen & Zhang, 2019).

The presence of protein and polysaccharide in the composite aerogels can be clearly observed at the wavenumbers of 1650–1200 cm^{-1} and 1051 cm^{-1} in the aerogel's spectra, respectively (Fig. 4c). The peak at a wavenumber of 1543.77 cm^{-1} in the protein spectrum (Amide II) has generally shifted to a higher wavenumber of 1558 cm^{-1} in the aerogels, which could be probably due to the formation of new hydrogen bonds between protein and polysaccharide, with the potential to increase the vibration frequency of N—H bending (Barth, 2007). The characteristic peak at 3457.66 cm^{-1} in gelatin, which was corresponded to OH groups' stretching, generally shifted to lower bands in the aerogels, demonstrating the improved hydrogen bonds in the systems (K. Chen & Zhang, 2019). Moreover, the absorption band at 1425 cm^{-1} in the QSG spectrum (COO^-) was disappeared in the gelatin/QSG aerogels spectra, probably due to electrostatic interactions between positively charged groups of gelatin and negatively charged (carboxyl) groups of QSG (Nooshkam et al., 2022). It could be generally concluded that both hydrogen and electrostatic interactions occurred between gelatin and QSG, which had remarkable effects on the structural and rheological properties of the composite hydrogels and aerogels.

3.2.4. DSC analysis

DSC is frequently used to evaluate structural changes of polysaccharides and proteins, in which the heating rate affects the location

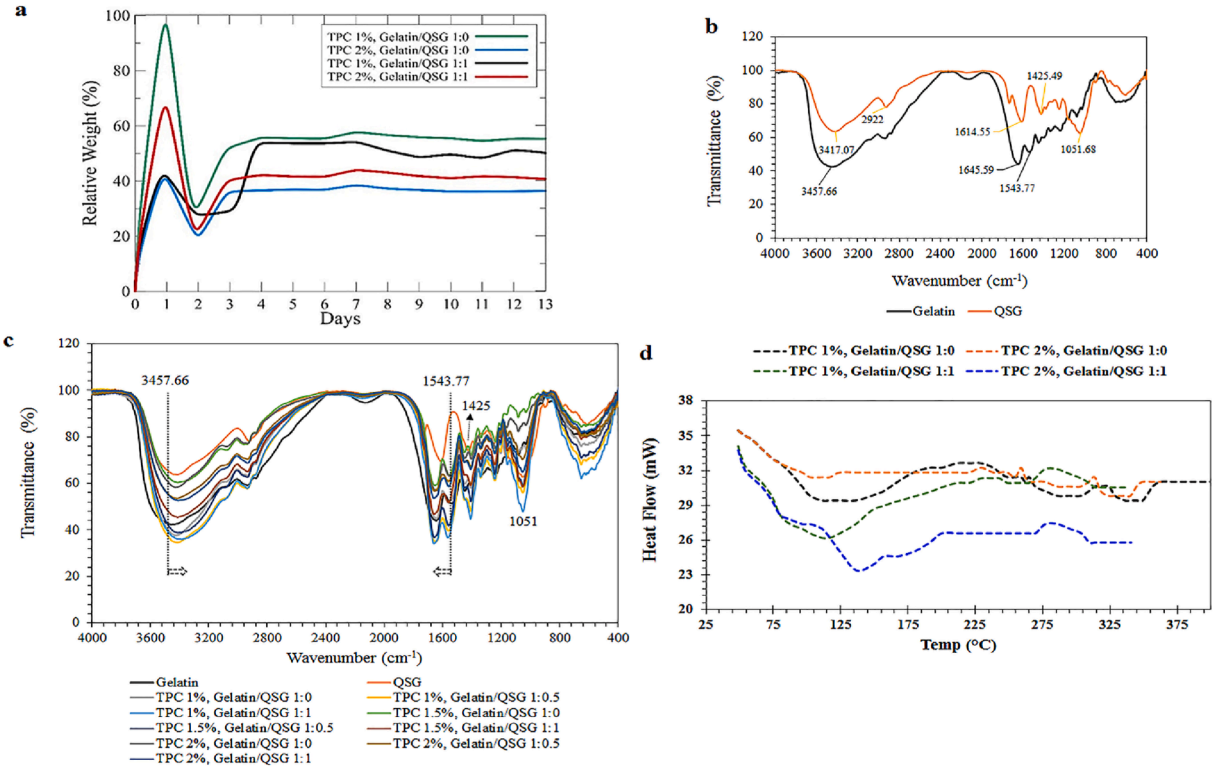

Fig. 4. Moisture absorption of gelatin/QSG composite aerogels (a), FTIR spectra of gelatin and QSG (b), FTIR spectra of gelatin/QSG composite aerogels (c), and thermograms of gelatin/QSG composite aerogels (d).

and shape of the peaks (Kazemi-Taskooh & Varidi, 2021). The first endothermic process for gelatin aerogels occurred at 70–80 °C (Fig. 4d), which may be due to the glass transition temperature (T_g) of the gelatin (Mukherjee & Rosolen, 2013). The observed peak at 76.85 °C could indicate the gelatin denaturation, which may relate to helix-to-random coils conversion that overlapped with T_g (Parvez et al., 2012).

Gelatin aerogels with TPC of 1% and 2% display characteristic peaks at 116.83 °C and 118.32 °C, respectively, which can be related to the melting temperature (T_m) of the gelatin (Mukherjee & Rosolen, 2013). In gelatin/QSG ratio of 1:1 with TPC of 1% and 2%, the peak temperature increased to 120.19 °C and 128.72 °C, correspondingly. Similarly, it has been reported that the T_m of gelatin increased after the addition of gellan and carrageenan (Fonkwe et al., 2003; Varghese et al., 2014). This means that the presence of polysaccharides could increase the thermal stability of proteins by modulating their denaturation behavior (S. Chen et al., 2018). The higher QSG concentrations (i.e., 1:1 gelatin/QSG ratio compared to 1:0 gelatin/QSG ratio) could increase the total negative net charge of the corresponding system and, in turn, its thermal stability (Kazemi-Taskooh & Varidi, 2021). Additionally, it was claimed that more gum concentration increased the endothermic peak temperature of the related gels (Watase & Nishinari, 1993). The peaks observed at 230–260 °C could be ascribed to the thermal decomposition of the samples. In line with our study, the thermal decomposition of gelatin films has been observed at the same temperature range (Fraga &

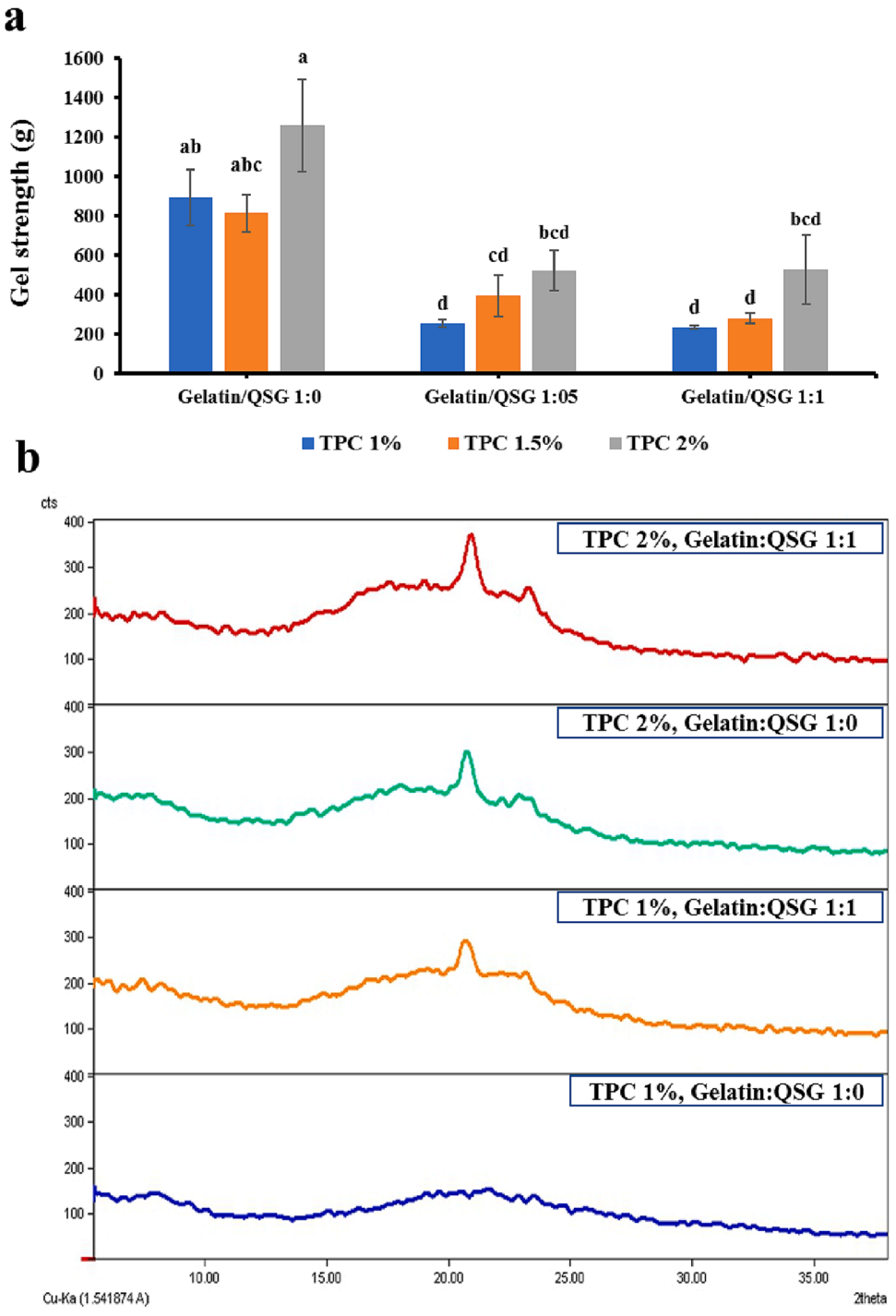

Fig. 5. Gel strength (a) and XRD patterns (b) of gelatin/QSG aerogels.

Williams, 1985).

3.2.5. Aerogel texture

The gel strength of gelatin/QSG composite aerogels increased significantly from an average of 459.57 g to 769.09 g as the TPC rose from 1% to 2% (Fig. 5a). Electrostatic interactions between $–NH_3$ groups in gelatin and –COOH groups in gum cause intermolecular crosslinks (Abhari, Madadlou, & Dini, 2017). This could lead to the formation of interconnected gel networks in the composite aerogels and, in turn, a harder texture. In corroborating our results, Jaberi, Pedram Nia, Naji-Tabasi, Elhamirad, and Shafafi Zenoozian (2020) argued that the higher protein-polysaccharide concentration provided an aerogel with a harder network structure than the low concentrations. Reducing gelatin/QSG ratio from 1:0 to 1:1 led to a marked decrease in gel strength ($p < 0.05$), most probably due to the ability of QSG to provide a more porous network with weaker walls in the aerogels (Section 3.2.1). The aerogels had remarkably higher gel strength values compared to corresponding hydrogels (~229.70%), which is attributed to the drying-derived extensive texture tightening effect (Ahmadi et al., 2016).

3.2.6. XRD studies

The XRD patterns of gelatin/QSG aerogels are indicated in Fig. 5b. A weak peak was observed at around $2\theta = 9^\circ$ for aerogel samples. Moreover, the aerogels had the main diffraction peaks around $2\theta = 21^\circ$, which is ascribed to the amorphous phase of proteins (Babaei et al., 2019b). The lack of sharpness in the diffraction peak around $2\theta = 21^\circ$ in the gelatin aerogels with 1% TPC suggests that the amorphous phase of proteins in the sample is less organized or exhibits a higher degree of disorder. This could be attributed to factors such as the lower concentration of gelatin, which may result in weaker protein–protein interactions and less ordered protein structure. The corresponding peak became markedly sharper as the TPC and QSG concentration increased in the aerogels, which could be an indication of more order, crystallization, and arrangement of the polymer's network (Dongol, El-Denglawey, Abd El Sadek, & Yahia, 2015). This may be most probably due to the decreased chain mobility of polymers (Frone, Berlioz, Chailan, & Panaitescu, 2013). The improved crystallinity of the binary aerogels can indicate their higher thermal stability, as confirmed by DSC results (Section 3.2.4). Moreover, the enhancement of aerogel crystallinity could be associated with the harder texture of the binary aerogels (Zhang et al., 2012). In agreement with our study, the characteristic diffraction peaks of gelatin have been reported to be observed around $2\theta = 8^\circ$ and 20° (Ki et al., 2005; Nagahama et al., 2009).

4. Conclusion

This study showed that adding certain levels of QSG to gelatin solution could provide composite hydrogels (and aerogels) with tailored functionality. It was demonstrated that gelatin/QSG hydrogels had lower syneresis values than gelatin hydrogels. However, excess QSG levels led to composite hydrogels with decreased gel strength and elasticity. The composite gelatin/QSG aerogels had greater gel strength than the corresponding hydrogels. Moreover, the improved thermal properties and porous network of the composite aerogel could make it a good candidate for efficient nutrient (bioactive) transfer and gaseous exchange in food and tissue engineering applications, especially as a carrier for aromatic compounds. However, the technofunctional and economic considerations of this promising aerogel should be evaluated in subsequent studies.

CRediT authorship contribution statement

Saba Ahmadzadeh-Hashemi: Methodology, Investigation, Resources, Writing – original draft, Software. **Mehdi Varidi:** Supervision, Funding acquisition, Conceptualization, Methodology, Visualization, Validation, Writing – review & editing. **Majid Nooshkam:** Visualization, Writing – original draft, Writing – review & editing.

Declaration of Competing Interest

The authors declare that they have no known competing financial interests or personal relationships that could have appeared to influence the work reported in this paper.

Data availability

Data will be made available on request.

Acknowledgments

This study was supported financially by Ferdowsi University of Mashhad (Grant No. 3/52787). The authors are also highly thankful to Gelatin Halal Pharmaceutical Processing Co. (Qazvin, Iran).

Appendix A. Supplementary data

Supplementary data to this article can be found online at https://doi.org/10.1016/j.fochx.2023.100813.

References

Abebe, W., & Ronda, F. (2014). Rheological and textural properties of tef [Eragrostis tef (Zucc.) Trotter] grain flour gels. *Journal of Cereal Science, 60*(1), 122–130. https://doi.org/10.1016/j.jcs.2014.02.001

Abhari, N., Madadlou, A., & Dini, A. (2017). Structure of starch aerogel as affected by crosslinking and feasibility assessment of the aerogel for an anti-fungal volatile release. *Food Chemistry, 221*, 147–152. https://doi.org/10.1016/j.foodchem.2016.10.072

Acar, H., & Kurt, A. (2020). Purified salep glucomannan synergistically interacted with xanthan gum: Rheological and textural studies on a novel pH-/thermo-sensitive hydrogel. *Food Hydrocolloids, 101*, Article 105463. https://doi.org/10.1016/j.foodhyd.2019.105463

Ahmadi, M., Madadlou, A., & Saboury, A. A. (2016). Whey protein aerogel as blended with cellulose crystalline particles or loaded with fish oil. *Food Chemistry, 196*, 1016–1022. https://doi.org/10.1016/j.foodchem.2015.10.031

Arboleda, J. C., Hughes, M., Lucia, L. A., Laine, J., Ekman, K., & Rojas, O. J. (2013). Soy protein–nanocellulose composite aerogels. *Cellulose, 20*(5), 2417–2426. https://doi.org/10.1007/s10570-013-9993-4

Ashraf, M. U., Hussain, M. A., Muhammad, G., Haseeb, M. T., Bashir, S., Hussain, S. Z., & Hussain, I. (2017). A superporous and superabsorbent glucuronoxylan hydrogel from quince (Cydonia oblanga): Stimuli responsive swelling, on-off switching and drug release. *International Journal of Biological Macromolecules, 95*, 138–144. https://doi.org/10.1016/j.ijbiomac.2016.11.057

Babaei, J., Khodaiyan, F., & Mohammadian, M. (2019a). Effects of enriching with gellan gum on the structural, functional, and degradation properties of egg white heat-induced hydrogels. *International Journal of Biological Macromolecules, 128*, 94–100. https://doi.org/10.1016/j.ijbiomac.2019.01.116

Babaei, J., Mohammadian, M., & Madadlou, A. (2019b). Gelatin as texture modifier and porogen in egg white hydrogel. *Food Chemistry, 270*, 189–195. https://doi.org/10.1016/j.foodchem.2018.07.109

Barth, A. (2007). Infrared spectroscopy of proteins. *Biochimica et Biophysica Acta (BBA)-Bioenergetics, 1767*(9), 1073–1101. https://doi.org/10.1016/j.bbabio.2007.06.004

Bashash, M., Varidi, M., & Varshosaz, J. (2022). Ultrasound-triggered transglutaminase-catalyzed egg white-bovine gelatin composite hydrogel: Physicochemical and rheological studies. *Innovative Food Science & Emerging Technologies, 76*, Article 102936. https://doi.org/10.1016/j.ifset.2022.102936

Binsi, P. K., Nayak, N., Sarkar, P. C., Joshy, C. G., Ninan, G., & Ravishankar, C. N. (2017). Gelation and thermal characteristics of microwave extracted fish gelatin-natural gum composite gels. *Journal of Food Science and Technology, 54*(2), 518–530. https://doi.org/10.1007/s13197-017-2496-9

Buisson, P., Hernandez, C., Pierre, M., & Pierre, A. C. (2001). Encapsulation of lipases in aerogels. *Journal of Non-Crystalline Solids, 285*(1), 295–302. https://doi.org/10.1016/S0022-3093(01)00470-7

Butler, M. F., & Heppenstall-Butler, M. (2003). Phase separation in gelatin/dextran and gelatin/maltodextrin mixtures. *Food Hydrocolloids, 17*(6), 815–830. https://doi.org/10.1016/S0268-005X(03)00103-6

Chandra, M. V., & Shamasundar, B. A. (2015). Texture Profile Analysis and Functional Properties of Gelatin from the Skin of Three Species of Fresh Water Fish. *International Journal of Food Properties, 18*(3), 572–584. https://doi.org/10.1080/10942912.2013.845787

Chen, K., & Zhang, H. (2019). Alginate/pectin aerogel microspheres for controlled release of proanthocyanidins. *International Journal of Biological Macromolecules, 136*, 936–943. https://doi.org/10.1016/j.ijbiomac.2019.06.138

Chen, S., Sun, C., Wang, Y., Han, Y., Dai, L., Abliz, A., & Gao, Y. (2018). Quercetagetin-loaded composite nanoparticles based on zein and hyaluronic acid: formation, characterization, and physicochemical stability. *Journal of Agricultural and Food Chemistry, 66*(28), 7441–7450. https://doi.org/10.1021/acs.jafc.8b01046

de Carvalho, R. A., & Grosso, C. R. F. (2004). Characterization of gelatin based films modified with transglutaminase, glyoxal and formaldehyde. *Food Hydrocolloids, 18*(5), 717–726. https://doi.org/10.1016/j.foodhyd.2003.10.005

de Oliveira, J. P., Bruni, G. P., el Halal, S. L. M., Bertoldi, F. C., Dias, A. R. G., & Zavareze, E.d. R. (2019). Cellulose nanocrystals from rice and oat husks and their application in aerogels for food packaging. *International Journal of Biological Macromolecules, 124*, 175–184. https://doi.org/10.1016/j.ijbiomac.2018.11.205

Derkach, S. R., Ilyin, S. O., Maklakova, A. A., Kulichikhin, V. G., & Malkin, A. Y. (2015). The rheology of gelatin hydrogels modified by κ-carrageenan. *LWT - Food Science and Technology, 63*(1), 612–619. https://doi.org/10.1016/j.lwt.2015.03.024

Derkach, S. R., Kuchina, Y. A., Kolotova, D. S., & Voron'ko, N. G. (2020). Polyelectrolyte polysaccharide-gelatin complexes: rheology and structure. *Polymers, 12*(2). https://doi.org/10.3390/polym12020266

Dongol, M., El-Denglawey, A., Abd El Sadek, M. S., & Yahia, I. S. (2015). Thermal annealing effect on the structural and the optical properties of Nano CdTe films. *Optik, 126*(14), 1352–1357. https://doi.org/10.1016/j.ijleo.2015.04.048

Farahmand, A., Varidi, M., & Koocheki, A. (2016). Investigation of functional properties of quince seed mucilage extracted by ultrasound. *Iranian Food Science and Technology Research Journal, 12*(1), 163–181. https://doi.org/10.22067/ifstrj.v1395i1.40595

Fennema, O. R., Damodaran, S., & Parkin, K. L. (2017). Introduction to food chemistry. In *Fennema's food chemistry* (pp. 1–16). CRC Press.

Fonkwe, L. G., Narsimhan, G., & Cha, A. S. (2003). Characterization of gelation time and texture of gelatin and gelatin–polysaccharide mixed gels. *Food Hydrocolloids, 17*(6), 871–883. https://doi.org/10.1016/S0268-005X(03)00108-5

Fraga, A. N., & Williams, R. J. J. (1985). Thermal properties of gelatin films. *Polymer, 26*(1), 113–118. https://doi.org/10.1016/0032-3861(85)90066-7

Frone, A. N., Berlioz, S., Chailan, J.-F., & Panaitescu, D. M. (2013). Morphology and thermal properties of PLA–cellulose nanofibers composites. *Carbohydrate Polymers, 91*(1), 377–384. https://doi.org/10.1016/j.carbpol.2012.08.054

García-González, C. A., Uy, J. J., Alnaief, M., & Smirnova, I. (2012). Preparation of tailor-made starch-based aerogel microspheres by the emulsion-gelation method. *Carbohydrate Polymers, 88*(4), 1378–1386. https://doi.org/10.1016/j.carbpol.2012.02.023

Ghadermazi, R., Khosrowshahi Asl, A., & Tamjidi, F. (2019). Optimization of whey protein isolate-quince seed mucilage complex coacervation. *International Journal of Biological Macromolecules, 131*, 368–377. https://doi.org/10.1016/j.ijbiomac.2019.03.026

Gilsenan, P. M., Richardson, R. K., & Morris, E. R. (2003). Associative and segregative interactions between gelatin and low-methoxy pectin: Part 1. Associative interactions in the absence of Ca2+. *Food Hydrocolloids, 17*(6), 723–737. https://doi.org/10.1016/S0268-005X(03)00094-8

Gómez-Guillén, M. C., Turnay, J., Fernández-Díaz, M. D., Ulmo, N., Lizarbe, M. A., & Montero, P. (2002). Structural and physical properties of gelatin extracted from different marine species: A comparative study. *Food Hydrocolloids, 16*(1), 25–34. https://doi.org/10.1016/S0268-005X(01)00035-2

Guzelgulgen, M., Ozkendir-Inanc, D., Yildiz, U. H., & Arslan-Yildiz, A. (2021). Glucuronoxylan-based quince seed hydrogel: A promising scaffold for tissue engineering applications. *International Journal of Biological Macromolecules, 180*, 729–738. https://doi.org/10.1016/j.ijbiomac.2021.03.096

Huang, T., Tu, Z., Shangguan, X., Wang, H., Zhang, L., & Bansal, N. (2021). Characteristics of fish gelatin-anionic polysaccharide complexes and their applications in yoghurt: Rheology and tribology. *Food Chemistry, 343*, Article 128413. https://doi.org/10.1016/j.foodchem.2020.128413

Jaberi, R., Pedram Nia, A., Naji-Tabasi, S., Elhamirad, A. H., & Shafafi Zenoozian, M. (2020). Rheological and structural properties of oleogel base on soluble complex of egg white protein and xanthan gum. *Journal of Texture Studies, 51*(6), 925–936. https://doi.org/10.1111/jtxs.12552

Kačuráková, M., Capek, P., Sasinková, V., Wellner, N., & Ebringerová, A. (2000). FT-IR study of plant cell wall model compounds: Pectic polysaccharides and hemicelluloses. *Carbohydrate Polymers, 43*(2), 195–203. https://doi.org/10.1016/S0144-8617(00)00151-X

Kasapis, S., Mitchell, J., Abeysekera, R., & MacNaughtan, W. (2004). Rubber-to-glass transitions in high sugar/biopolymer mixtures. *Trends in Food Science & Technology, 15*(6), 298–304. https://doi.org/10.1016/j.tifs.2003.09.021

Kazemi-Taskooh, Z., & Varidi, M. (2021). Designation and characterization of cold-set whey protein-gellan gum hydrogel for iron entrapment. *Food Hydrocolloids, 111*, Article 106205. https://doi.org/10.1016/j.foodhyd.2020.106205

Ki, C. S., Baek, D. H., Gang, K. D., Lee, K. H., Um, I. C., & Park, Y. H. (2005). Characterization of gelatin nanofiber prepared from gelatin–formic acid solution. *Polymer, 46*(14), 5094–5102. https://doi.org/10.1016/j.polymer.2005.04.040

Kleemann, C., Selmer, I., Smirnova, I., & Kulozik, U. (2018). Tailor made protein based aerogel particles from egg white protein, whey protein isolate and sodium caseinate: Influence of the preceding hydrogel characteristics. *Food Hydrocolloids, 83*, 365–374. https://doi.org/10.1016/j.foodhyd.2018.05.021

Le, X. T., & Turgeon, S. L. (2013). Rheological and structural study of electrostatic cross-linked xanthan gum hydrogels induced by β-lactoglobulin. *Soft Matter, 9*(11), 3063–3073. https://doi.org/10.1039/C3SM27528K

Lee, K. Y., Shim, J., Bae, I. Y., Cha, J., Park, C. S., & Lee, H. G. (2003). Characterization of gellan/gelatin mixed solutions and gels. *LWT - Food Science and Technology, 36*(8), 795–802. https://doi.org/10.1016/S0023-6438(03)00116-6

Liu, Y., Weng, R., Wang, W., Wei, X., Li, J., Chen, X., … Li, Y. (2020). Tunable physical and mechanical properties of gelatin hydrogel after transglutaminase crosslinking on two gelatin types. *International Journal of Biological Macromolecules, 162*, 405–413. https://doi.org/10.1016/j.ijbiomac.2020.06.185

Manrique, G. D., & Lajolo, F. M. (2002). FT-IR spectroscopy as a tool for measuring degree of methyl esterification in pectins isolated from ripening papaya fruit. *Postharvest Biology and Technology, 25*(1), 99–107. https://doi.org/10.1016/S0925-5214(01)00160-0

Martin, A. H., Bakhuizen, E., Ersch, C., Urbonaite, V., de Jongh, H. H. J., & Pouvreau, L. (2016). Gelatin increases the coarseness of whey protein gels and impairs water exudation from the mixed gel at low temperatures. *Food Hydrocolloids, 56*, 236–244. https://doi.org/10.1016/j.foodhyd.2015.12.019

Mikkonen, K. S., Parikka, K., Ghafar, A., & Tenkanen, M. (2013). Prospects of polysaccharide aerogels as modern advanced food materials. *Trends in Food Science & Technology, 34*(2), 124–136. https://doi.org/10.1016/j.tifs.2013.10.003

Mohtar, N. F., Perera, C. O., Quek, S.-Y., & Hemar, Y. (2013). Optimization of gelatine gel preparation from New Zealand hoki (Macruronus novaezelandiae) skins and the effect of transglutaminase enzyme on the gel properties. *Food Hydrocolloids, 31*(2), 204–209. https://doi.org/10.1016/j.foodhyd.2012.10.011

Mukherjee, I., & Rosolen, M. (2013). Thermal transitions of gelatin evaluated using DSC sample pans of various seal integrities. *Journal of Thermal Analysis and Calorimetry, 114*(3), 1161–1166. https://doi.org/10.1007/s10973-013-3166-4

Nagahama, H., Maeda, H., Kashiki, T., Jayakumar, R., Furuike, T., & Tamura, H. (2009). Preparation and characterization of novel chitosan/gelatin membranes using chitosan hydrogel. *Carbohydrate Polymers, 76*(2), 255–260. https://doi.org/10.1016/j.carbpol.2008.10.015

Nooshkam, M., & Varidi, M. (2020). Whey protein isolate-low acyl gellan gum Maillard-based conjugates with tailored technological functionality and antioxidant activity. *International Dairy Journal, 109*, Article 104783. https://doi.org/10.1016/j.idairyj.2020.104783

Nooshkam, M., Varidi, M., & Alkobeisi, F. (2022). Bioactive food foams stabilized by licorice extract/whey protein isolate/sodium alginate ternary complexes. *Food Hydrocolloids, 126*, Article 107488. https://doi.org/10.1016/j.foodhyd.2022.107488

Pan, J., Li, Y., Chen, K., Zhang, Y., & Zhang, H. (2021). Enhanced physical and antimicrobial properties of alginate/chitosan composite aerogels based on electrostatic interactions and noncovalent crosslinking. *Carbohydrate Polymers, 266*, Article 118102. https://doi.org/10.1016/j.carbpol.2021.118102

Parvez, S., Rahman, M. M., Khan, M. A., Khan, M. A. H., Islam, J. M. M., Ahmed, M., … Ahmed, B. (2012). Preparation and characterization of artificial skin using chitosan and gelatin composites for potential biomedical application. *Polymer Bulletin, 69*(6), 715–731. https://doi.org/10.1007/s00289-012-0761-7

Petcharat, T., & Benjakul, S. (2017). Property of fish gelatin gel as affected by the incorporation of gellan and calcium chloride. *Food Biophysics, 12*(3), 339–347. https://doi.org/10.1007/s11483-017-9489-0

Pires Vilela, J. A., Cavallieri, Â. L. F., & Lopes da Cunha, R. (2011). The influence of gelation rate on the physical properties/structure of salt-induced gels of soy protein isolate–gellan gum. *Food Hydrocolloids, 25*(7), 1710–1718. https://doi.org/10.1016/j.foodhyd.2011.03.012

Rezagholi, F., Hashemi, S. M. B., Gholamhosseinpour, A., Sherahi, M. H., Hesarinejad, M. A., & Ale, M. T. (2019). Characterizations and rheological study of the purified polysaccharide extracted from quince seeds. *Journal of the Science of Food and Agriculture, 99*(1), 143–151. https://doi.org/10.1002/jsfa.9155

Sasahara, K., McPhie, P., & Minton, A. P. (2003). Effect of dextran on protein stability and conformation attributed to macromolecular crowding. *Journal of Molecular Biology, 326*(4), 1227–1237. https://doi.org/10.1016/S0022-2836(02)01443-2

Sow, L. C., Nicole Chong, J. M., Liao, Q. X., & Yang, H. (2018). Effects of κ-carrageenan on the structure and rheological properties of fish gelatin. *Journal of Food Engineering, 239*, 92–103. https://doi.org/10.1016/j.jfoodeng.2018.05.035

Sun, Y., Zheng, J., Tong, Y., Wu, Y., Liu, X., Niu, L., & Li, H. (2022). Construction of three-dimensional nitrogen doped porous carbon flake electrodes for advanced potassium-ion hybrid capacitors. *Journal of Colloid and Interface Science, 606*, 1940–1949. https://doi.org/10.1016/j.jcis.2021.09.143

Tolstoguzov, V. B. (1995). Some physico-chemical aspects of protein processing in foods. Multicomponent gels. *Food Hydrocolloids, 9*(4), 317–332. https://doi.org/10.1016/S0268-005X(09)80262-2

Varghese, J. S., Chellappa, N., & Fathima, N. N. (2014). Gelatin–carrageenan hydrogels: Role of pore size distribution on drug delivery process. *Colloids and Surfaces B: Biointerfaces, 113*, 346–351. https://doi.org/10.1016/j.colsurfb.2013.08.049

Vignon, M. R., & Gey, C. (1998). Isolation, 1H and 13C NMR studies of (4-O-methyl-d-glucurono)-d-xylans from luffa fruit fibres, jute bast fibres and mucilage of quince tree seeds. *Carbohydrate Research, 307*(1), 107–111. https://doi.org/10.1016/S0008-6215(98)00002-0

Wang, L., Liu, H. M., Xie, A. J., Wang, X. D., Zhu, C. Y., & Qin, G. Y. (2018). Chinese quince (Chaenomeles sinensis) seed gum: Structural characterization. *Food Hydrocolloids*, 237–245.

Watase, M., & Nishinari, K. (1993). Effect of potassium ions on the rheological and thermal properties of gellan gum gels. *Food Hydrocolloids, 7*(5), 449–456. https://doi.org/10.1016/S0268-005X(09)80240-3

Wu, B.-C., Degner, B., & McClements, D. J. (2014). Soft matter strategies for controlling food texture: Formation of hydrogel particles by biopolymer complex coacervation. *Journal of Physics: Condensed Matter, 26*(46), Article 464104. https://doi.org/10.1088/0953-8984/26/46/464104

Yadav, S., Mehrotra, G. K., Bhartiya, P., Singh, A., & Dutta, P. K. (2020). Preparation, physicochemical and biological evaluation of quercetin based chitosan-gelatin film

for food packaging. *Carbohydrate Polymers, 227*, Article 115348. https://doi.org/10.1016/j.carbpol.2019.115348

Yun, L., Zhao, J., Kang, X., Du, Y., Yuan, X., & Hou, X. (2017). Preparation and properties of monolithic and hydrophobic gelatin–silica composite aerogels for oil absorption. *Journal of Sol-Gel Science and Technology, 83*(1), 197–206. https://doi.org/10.1007/s10971-017-4378-z

Zhang, H., Xia, H., & Zhao, Y. (2012). Poly(vinyl alcohol) hydrogel can autonomously self-heal. *ACS Macro Letters, 1*(11), 1233–1236. https://doi.org/10.1021/mz300451r